Published in final edited form as:
Cell Host Microbe. 2013 August 14; 14(2): 159–170. doi:10.1016/j.chom.2013.07.009.

PPARγ-mediated increase in glucose availability sustains chronic *Brucella abortus* infection in alternatively activated macrophages

Mariana N. Xavier[1,2], **Maria G. Winter**[1,*], **Alanna M. Spees**[1,*], **Andreas B. den Hartigh**[1], **Kim Nguyen**[1], **Christelle M. Roux**[1], **Teane M. A. Silva**[2], **Vidya L. Atluri**[1], **Tobias Kerrinnes**[1], **A. Marijke Keestra**[1], **Denise M. Monack**[4], **Paul A. Luciw**[3], **Richard A. Eigenheer**[5], **Andreas J. Bäumler**[1], **Renato L. Santos**[2], and **Renée M. Tsolis**[1,#]

[1]Department of Medical Microbiology and Immunology, School of Medicine, University of California at Davis, Davis, CA, 95616, USA

[2]Departamento de Clinica e Cirurgia Veterinarias, Escola de Veterinaria, Universidade Federal de Minas Gerais, 31270-901 Belo Horizonte, MG, Brazil

[3]Center for Comparative Medicine, University of California at Davis, Davis, CA, 95616, USA

[4]Department of Microbiology & Immunology, School of Medicine, Stanford University, Palo Alto, CA, 94305, USA

[5]Proteomics Core Facility, University of California at Davis Genome Center, Davis, CA, 95616, USA

SUMMARY

Eradication of persistent intracellular bacterial pathogens with antibiotic therapy is often slow or incomplete. However, strategies to augment antibiotics are hampered by our poor understanding of the nutritional environment that sustains chronic infection. Here we show that the intracellular pathogen *Brucella abortus* survives and replicates preferentially in alternatively activated macrophages (AAM), which are more abundant during chronic infection. A metabolic shift induced by peroxisome proliferator activated receptor γ (PPARγ), which increases intracellular glucose availability, is identified as a causal mechanism promoting enhanced bacterial survival in AAM. Glucose uptake was crucial for increased replication of *B. abortus* in AAM, and chronic infection, as inactivation of the bacterial glucose transporter *gluP* reduced both intracellular survival in AAM and persistence in mice. Thus, a shift in intracellular nutrient availability induced by PPARγ promotes chronic persistence of *B. abortus* within AAM and targeting this pathway may aid in eradicating chronic infection.

INTRODUCTION

Brucella abortus is a zoonotic bacterial pathogen that establishes long-term infections in its host. *In vivo*, bacteria are found in association with phagocytic cells, most prominently

[#]Correspondence: Renee M. Tsolis, PhD, Department of Medical Microbiology and Immunology, University of California, Davis; Davis, California 95616, rmtsolis@ucdavis.edu, Fax: 530-754-7240, Phone: 530-754-8497.
[*]These authors contributed equally.

macrophages, in which a subset of *B. abortus* is able to evade killing in phagolysosomes. Instead, bacteria replicate with an endoplasmic reticulum-associated compartment and interact subsequently with a modified autophagy pathway to promote cell-to cell spread (Gorvel and Moreno, 2002; Starr et al., 2008). While studies on the interaction between *B. abortus* and macrophages have yielded critical insights into how *B. abortus* survives intracellularly, a subset of factors required for chronic persistence *in vivo* do not appear to mediate intracellular replication in cultured macrophages (Fretin et al., 2005; Hong et al., 2000), raising the possibility that the niche for chronic bacterial persistence has different characteristics from macrophages cultured *in vitro*.

Recently, it has been recognized that like other immune cells, macrophages can adopt different functional states that are influenced by the immune microenvironment [reviewed by (Gordon and Martinez, 2010; Van Dyken and Locksley, 2013)]. Activation by interferon gamma (IFNγ) leads to the classically activated macrophage (CAM) phenotype, characterized by production of nitric oxide (NO) and inflammatory cytokines such as tumor necrosis factor alpha (TNFα) and interleukin 6 (IL-6). During inflammation, these cells can arise from $Ly6C^{high}$ inflammatory monocytes that leave the bone marrow in a CCR2-dependent manner (Shi and Pamer, 2011). In contrast, the Th2 cytokines interleukin-4 (IL-4) and IL-13 activate signal transducer and activator of transcription 6 (STAT6) to promote development of alternatively activated macrophages (AAM), which play important roles in allergic inflammation, helminth infection and tissue repair (Lawrence and Natoli, 2011; Reyes and Terrazas, 2007; Shirey et al., 2008). These macrophages express low levels of the inflammatory monocyte marker LY6C.

In addition to roles in inflammation and immunity, CAM and AAM play important roles in host physiology and metabolism (reviewed by (Chawla, 2010). Development of the AAM phenotype is dependent on peroxisome proliferator activated receptors (PPARs; (Odegaard et al., 2007), which act downstream of STAT6 signaling to regulate macrophage metabolism. Interestingly, our previous results (Hong et al., 2000) implicated bacterial metabolism as key to chronic *B. abortus* infection. Therefore, we sought to investigate the relative importance of AAM and CAM as niches for persistent infection, and to determine whether the different metabolic programming of these two macrophage populations contributes to chronic infection by *B. abortus*.

RESULTS

Alternatively activated macrophages are more abundant during chronic *B. abortus* infection compared to acute infection

To gain insight into the role of different macrophage populations during different phases of *B. abortus* infection, we performed an infection time course experiment. These results showed that early (1–3d) bacterial numbers increased, then subsequently declined over the next 21 days, and we designated this as the acute phase of infection. Between 30 and 60 days post infection, bacterial numbers remained constant, and this was designated the chronic infection phase (Fig. 1A). During the acute phase of infection, a short-lived Th1 response (Fernandes et al., 1996) and an influx of inflammatory macrophages (Copin et al., 2012) act to control bacterial colonization. However, while *B. abortus* is found within CAM early during infection, the intracellular niche for *B. abortus* during the persistence phase is unknown. To shed light on this question, we compared expression of markers of AAM (Fig. 1 and Fig S1) and CAM (Fig. S1) in the spleen, a site of systemic *B. abortus* persistence, during acute and chronic infection. While markers of classical macrophage activation, such as *Nos2* (encoding inducible nitric oxide synthase), *Il6* (encoding interleukin-6), and *Tnfa* (encoding tumor necrosis factor alpha), were elevated in splenic macrophages ($CD11b^+$ cells) during the acute phase of infection, expression of these markers declined during

persistent infection (Fig S1A). Further, while the total number of macrophages in the spleen was increased in both acute and chronic infection compared to uninfected mice (Fig. 1B), a significantly greater proportion of these macrophages had an inflammatory phenotype during acute infection, as evidenced by their Ly6C^{high} phenotype (Figs. 1C and 1E), and low expression of AAM markers *Ym1* and *Fizz1* (Fig. S1B and S1C). Ly6C^{high} monocytes contributed to control of *B. abortus* infection during the acute phase, since mice deficient for the C-C chemokine receptor 2 (*Ccr2*$^{-/-}$ mice), which are deficient for egress of Ly6C^{high} monocytes from the bone marrow, were colonized ~3 fold more highly during the acute phase (9d) of infection (Fig. S1D). Macrophages from *B. abortus*-infected *Ccr2*$^{-/-}$ mice also had reduced levels of inflammatory markers and increased expression of AAM markers (Fig. S1E), suggesting that increased numbers of AAM in the *Ccr2*$^{-/-}$ mice may contribute to the increased *B. abortus* colonization observed in these mice.

In contrast to acute *B. abortus* infection, during the chronic infection phase (30d), flow cytometric analysis of splenic macrophages (CD3^{-}B220^{-}NK1.1^{-}Ly6G^{-}CD11b^{+}F4/80^{+} cells) revealed an increase in cells with a Ly6C^{low} phenotype that were positive for the AAM marker CD301 (Fig. 1D–F). In addition, higher expression levels of the AAM markers *Ym1* and *Fizz1* (encoding proteins secreted by AAM) were observed, suggesting an increased abundance of AAM at this time point (Fig. S1B). Immunohistochemical analysis of Ym1 and Fizz1 expression in splenic tissue confirmed that while these AAM markers were expressed at low levels in uninfected and acutely infected spleen tissue, the abundance of both markers was elevated during chronic infection, at day 30 (Fig. S1C). Together these lines of evidence provided support for the idea that AAM are more abundant in the spleen during the chronic infection phase of brucellosis, and suggested that AAM may provide a niche for persistence of *B. abortus*.

AAM support increased levels of intracellular *B. abortus* replication

To determine whether AAM could be a preferred niche for *B. abortus*, we quantified bacterial survival and replication in bone marrow-derived macrophages (BMDM) that were unstimulated, treated with interferon gamma (IFNγ) to produce CAM or treated with interleukin-4 (IL-4) to produce AAM (Fig. 2A). As expected, BMDM responded to IL-4 with increased expression of *Ym1, Fizz1* and *Il6*, while CAM expressed higher levels of *Il6* than AAM (data not shown). While the CAM eliminated intracellular *B. abortus* infection, both unstimulated BMDM and AAM were permissive for intracellular replication of *B. abortus* (Fig. 2A). Remarkably, *B. abortus* replicated to tenfold higher numbers in AAM than in untreated control BMDM, demonstrating an increased capacity of these cells to support intracellular infection (Fig. 2A).

To determine whether the AAM also serve as a preferential niche for *B. abortus* during chronic infection, we determined the intracellular localization of *B. abortus* by enrichment of CD11b^{+} cells and flow cytometry (Fig. 2). During the acute infection, *B. abortus* was recovered from both the CD11b^{+} and the CD11b^{-} cell fraction, consistent with a previous report (Copin et al., 2012). However during chronic infection, *B. abortus* localized predominantly to the CD11b^{+} fraction (Fig. 2B). Flow cytometric analysis of the CD11b^{+} fraction revealed that that during acute infection *B. abortus* localized to CD11b+ dendritic cells, as well as to macrophages that were Ly6C^{high} and Ly6C^{low} (Fig. 2C and 2D). In contrast, during chronic infection, *B. abortus* colocalized with macrophages that were Ly6C^{low}. Since AAM are described to express low levels of Ly6C as well as the marker CD301, we further analyzed the Ly6C^{low} population for expression of CD301 and found an approximately fivefold higher association of *B. abortus* with Ly6C^{low} CD301^{+} cells (AAM) than with Ly6C^{low} CD301^{-} cells (Fig. 2E). Together, these results demonstrated that *B. abortus* preferentially associated with AAM during chronic (but not acute) infection.

Since the results shown above suggested that AAM could be a niche for intracellular persistence of *B. abortus*, we tested whether mice with defects in generation of CAM (*Ifng*$^{-/-}$ mice) or AAM (*Stat6*$^{-/-}$ mice) would be altered in their ability to control *B. abortus* infection (Fig. 3). Consistent with findings of other groups, *Ifng*$^{-/-}$ mice were severely deficient in control of *B. abortus* infection during the acute phase, where bacterial numbers increased rapidly (Fig. 3A). This increased load of *B. abortus* correlated with an increase in the number of Ly6C^{low} CD301^{+} AAM (Fig. 3B and Fig. 3C). Compared to control (C57BL/6) mice, *Ifng*$^{-/-}$ mice expressed lower levels of the CAM markers *Il6* and *Nos2* and higher levels of the AAM marker *Ym1* in splenic macrophages during the acute infection phase (Fig. S2D). Moreover, immunohistochemical analysis confirmed increased levels of the AAM markers Ym1 and Fizz1 in spleens of *Ifng*$^{-/-}$ mice during acute infection (days 9 and 21) when compared to control mice (Fig. S2E, data not shown). These results suggested that IFNγ-deficiency resulted in an increase in numbers of AAM during the acute phase of *B. abortus* infection. Thus one important role of IFNγ in controlling *B. abortus* during the acute phase of infection may be to direct the differentiation of CAM. The opposite effect was seen in *Stat6*$^{-/-}$ mice, which demonstrated an increased ability to control *B. abortus* persistence during the chronic infection phase (30 dpi; Fig 3D). Increased control of *B. abortus* in these mice correlated with decreased expression of AAM markers and increased CAM marker expression in splenic macrophages, suggesting that a decrease in AAM polarization in the *Stat6*$^{-/-}$ mice contributes to their increased resistance to *B. abortus* infection (Fig 3E).

PPARγ promotes intracellular *B. abortus* replication in AAM

A pathway that is crucial to acquisition and maintenance of the AAM phenotype is mediated by peroxisome proliferator-activated receptors (PPARs), a family of nuclear receptors that regulates transcription of genes involved in cellular metabolism (Odegaard et al., 2007; Vats et al., 2006). Since our previous studies of *B. abortus* genes involved in persistent, but not acute infection, implicated metabolic genes in this process (Hong et al., 2000), we tested the hypothesis that PPAR-mediated changes to macrophage metabolism could provide an environment for intracellular persistence of *B. abortus*. To determine whether any of the PPARs could be involved in this process, we analyzed transcripts of the PPARs in splenic CD11b^{+} cells. Our results showed that transcription of *Pparg*, the gene encoding PPARγ, was reduced during acute infection compared to uninfected controls, while during chronic infection (30–60 days), it was elevated (Fig. 4A). Moreover, *Ifng*$^{-/-}$ mice had increased *Pparg* expression in splenic macrophages during acute infection while the opposite was true for chronically infected *Stat6*$^{-/-}$ mice when compared to control animals (data not shown). In *B. abortus*-infected mice, blocking of PPARγ activity by treating the mice with the inhibitor GW9662 specifically prior to chronic infection (days 18 until 30) led to a significant decrease in splenic colonization at 30 days after infection, suggesting that pathways downstream of PPARγ contribute to generating a niche for persistence of *B. abortus* (Fig. 4B). Concomitantly, PPARγ inhibition led to a reduction in the proportion of Ly6C^{low} CD301^{+} AAM in the spleen at 30 dpi (Fig. 4C), as well as to decreased expression of the AAM marker Ym1 and to increased expression levels of CAM gene *Nos2* and in splenic CD11b^{+} cells (Fig. S3A). These results suggested that inhibition of PPARγ reduced *B. abortus* survival by reducing the abundance of AAM during chronic infection (Fig. 4C).

Conversely, treatment of *B. abortus*-infected mice with the PPARγ agonist Rosiglitazone led to a small (twofold) increase in *B. abortus* colonization during the acute (9d) phase and a ~4 fold increase during the chronic (30d) infection phase (Fig. 4D). During the acute infection phase, Rosiglitazone treatment led to an increased percentage of Ly6C^{low}CD301^{+} macrophages (Fig. 4E), as well as a shift toward expression of AAM markers and a reduction in the CAM marker *Nos2* (Fig. S3B), suggesting that the increase in *B. abortus* infection in Rosiglitazone-treated mice resulted from a relative increase in AAM during the

acute phase of infection. Since systemic modulation of PPARγ activity could have effects on cells other than macrophages, we repeated these treatments on *in vitro* polarized AAM. Similar to what we observed *in vivo*, *Pparg* was strongly induced in AAM differentiated *in vitro* (Fig. 4F). Inhibition of PPARγ activity in AAM with GW9662 resulted in a decreased ability to support intracellular replication of *B. abortus*, while activation of PPARγ led to an additional increase in *B. abortus* replication (Fig 4G). Moreover, fluorescence microscopy analysis confirmed that increased *B. abortus* CFU counts in AAM and PPARγ stimulated macrophages were due to increased bacterial numbers within each cell, rather than a higher number of infected cells (Fig S3C). Together, these results suggest that PPARγ-dependent modulation of macrophage physiology promotes intracellular persistence of *B. abortus*.

PPARγ increases the availability of intracellular glucose in AAM

One of the metabolic changes mediated by PPARγ is a shift from oxidative metabolism of glucose to β-oxidation of fatty acids. Further, PPARγ agonists are used therapeutically to lower blood glucose by increasing cellular glucose uptake (Yki-Järvinen, 2004). Since *B. abortus* is able to utilize glucose for growth (McCullough and Beal, 1951) we tested the possibility that increased intracellular glucose availability could promote intracellular replication of *B. abortus* in AAM.

We first investigated whether *B. abortus* infection altered the phenotype of macrophages cultured *in vitro*. Infection of non-polarized macrophages with *B. abortus* or the closely related *B. melitensis* led to moderately increased abundance of glycolytic pathway enzymes (Fig. S4A), as well as an increase in expression of the CAM markers *Hifa*, *Pfkfb3* and *Glut1* (Fig. S4B). In contrast, *B. abortus* infection decreased expression of *Pgc1b*, encoding a transcriptional activator and *Acadm* and *Acadl*, encoding enzymes involved in mitochondrial β-oxidation (Fig. S4C). The induction of the glycolytic pathway in *B. abortus*-infected macrophages was confirmed by detection of increased concentrations of extracellular lactate, an end-product of glycolysis (Fig. S4D). The relative induction of the macrophage glycolytic pathway by *B. abortus* was dependent on the macrophage phenotype: infection of CAM (induced by IFNγ) or AAM (induced by IL-4) treated with the PPARγ antagonist GW9662 shifted the metabolism more strongly toward glycolysis and led to a marked reduction in β-oxidation genes expression (Figs. 5A–5C). In contrast, compared to control (untreated) macrophages, the shift toward glycolysis induced by *B. abortus* infection was attenuated in AAM or in cells treated with Rosiglitazone (Figs. 5A–5C). Taken together, these data suggested that while *B. abortus* infection does not induce AAM polarization, infection of AAM results in lower induction of the glycolytic pathway in the infected macrophages.

Compared to untreated control bone marrow-derived macrophages, AAM induced *in vitro* by IL-4 treatment had significantly elevated glucose content, which was lowered to the level of control macrophages by infection with *B. abortus,* raising the possibility that the pathogen may consume this carbon source (Fig. 5D). Increased intracellular glucose in AAM was recapitulated by treatment with Rosiglitazone, and was negated by treatment of AAM with GW9662, suggesting that increased intracellular glucose in AAM is dependent on PPARγ mediated transcriptional changes (Fig. 5D). Interestingly, our previous work identified a glucose transporter of the major facilitator superfamily, GluP, as a *B. abortus* factor required for chronic, but not acute, infection (Essenberg et al., 1997; Hong et al., 2000).

To directly test the idea that glucose availability could promote intracellular replication of *B. abortus* in AAM, we compared replication of wild type *B. abortus* and the *gluP* mutant. *In vitro*, the *gluP* mutant grew similarly to wild type *B. abortus* in medium (Tryptone/Soytone) lacking glucose, while addition of glucose enhanced replication of wild type *B. abortus*, but not of the *gluP* mutant (Fig. S5A). Enhanced growth in glucose-containing medium was

restored by complementation of the *gluP* mutation (Fig. S5A). Remarkably, while there was no difference in the ability of the two *B. abortus* strains to survive in untreated control macrophages, wild type *B. abortus* was recovered in tenfold greater numbers than the *gluP* mutant from AAM (Fig. 6A). Treatment of unpolarized BMDM with Rosiglitazone increased the intracellular replication of wild type *B. abortus*, but had no effect on intracellular replication of the *gluP* mutant, consistent with an inability to utilize increased glucose within the macrophage (Fig. 6B). The growth advantage of wild type *B. abortus* over the *gluP* mutant was eliminated by treatment of AAM with GW9662 (Fig. 6B). Inhibition of mitochondrial β-oxidation in AAM or Rosiglitazone-treated cells, using the carnitine palmitoyltransferase inhibitor etomoxir, also reduced the ability of *B. abortus* to replicate intracellularly, but had no effect on the *gluP* mutant (Fig. 6C and Fig. S5B). The growth defect of the *gluP* mutant within AAM or Rosiglitazone-treated macrophages was restored by complementation (Fig 6D and 6E), demonstrating that the ability to transport glucose is essential for increased growth in these macrophages. To control for possible off-target effects of the inhibitors on *B. abortus*, we examined replication of wild type and the *gluP* mutant in macrophages from conditionally PPARγ-deficient mice, in which only macrophages lack PPARγ (Figs. S5C and S5D). Similarly to what was observed with the PPARγ inhibitor-treated AAM (Fig. 6B), GluP-dependent replication of *B. abortus* within either IL-4 or Rosiglitazone-treated macrophages was dependent on the function of PPARγ (Figs. S5C and S5D). These results provide evidence that the increased replication of *B. abortus* in AAM is dependent on its ability to utilize the elevated intracellular pool of glucose that is induced by PPARγ.

Persistent infection by *B. abortus* depends on the ability to transport glucose

The results presented above raised the question, whether the PPARγ-dependent increase in glucose concentration that we observed in cultured macrophages could also promote *B. abortus* infection *in vivo*. To investigate this, we determined the requirement for GluP during acute and chronic infection (Fig. 7A), using a competitive infection assay. During acute infection (9 days) the ratio of wild type *B. abortus* to the *gluP* mutant was not significantly different from the 1:1 ratio in the inoculum (Fig. 7A). However during chronic infection, the *gluP* mutant was outcompeted 20-fold by the wild type. To determine whether this competitive defect was the result of PPARγ activation, we repeated the experiment in mice treated with the PPARγ antagonist GW9662 (Fig. 7B). Inhibition of PPARγ during the chronic infection stage strongly reduced the competitive defect of the *gluP* mutant at 30 dpi. Since the survival defect of the *gluP* mutant was observed only during chronic infection, when PPARγ expression was increased, we next asked whether activation of PPARγ during acute infection would affect the survival of the *gluP* mutant (Fig. 7C). Treatment of mice during acute infection with Rosiglitazone increased the ability of the wild type *B. abortus* to outcompete the *gluP* mutant at 9d by approximately four-fold, resembling the phenotype only previously seen at later stages of infection (30d). Finally, to control for off-target effects of the inhibitors, we repeated the competitive infection in mice conditionally deficient for *Pparg* expression in macrophages (*Pparg*$^{flox/flox}$ LysM$^{cre/-}$; (Odegaard et al., 2007)). The growth advantage of wild type *B. abortus* over the *gluP* mutant was strongly reduced in the conditionally *Pparg*-deficient mice (Fig. 7D), demonstrating that expression of PPARγ specifically in macrophages is required for *B. abortus* to benefit from acquisition of glucose in AAM during chronic infection. Taken together, these results demonstrate that, *in vivo*, the ability of *B. abortus* to benefit from PPARγ-mediated changes in host macrophage metabolism is dependent on the ability of *B. abortus* to take up glucose.

DISCUSSION

Recent studies have shed light on the extensive interactions between immune and metabolic functions of macrophages. For the case of CAM, oxygen is required as a substrate for NADPH oxidase, and therefore these cells meet their energetic needs via anaerobic glycolysis. Since anaerobic glucose utilization is a relatively inefficient way to generate ATP (only 2 ATP/molecule of glucose), a large amount of glucose must be utilized, and the relative intracellular concentration of free glucose is low. In contrast, in AAM, this metabolic program is antagonized by STAT6-dependent induction of PPARγ and PPARδ (Szanto et al., 2010). As a result, AAM shift to aerobic metabolism, in which they gain energy by β-oxidation of fatty acids (Bensinger and Tontonoz, 2008; O'Neill and Hardie, 2013). Our results demonstrate that this metabolic shift leads to an increase in intracellular glucose, which becomes available to support growth of intracellular bacteria (Fig. 5). An exhaustive screen of *B. suis* genes required for intracellular infection in human THP-1 cells identified sugar metabolism genes as being required for intracellular infection, and suggested that the replicative niche for *Brucella* within the cell is poor in nutrients (Kohler et al., 2002). Further, at late stages during cellular infection, the bacterial glycolysis pathway was downregulated, which led to the proposition that *Brucella* may use fatty acids or amino acids rather than sugars during this growth phase (Al Dahouk et al., 2008; Barbier et al., 2011). However, the increased growth rate of *B. abortus* within AAM *in vitro* compared to unpolarized or CAM-polarized macrophage populations used for previous studies suggests that AAM may provide additional nutrients, such as glucose, that are less abundant in other macrophage populations.

Like *B. abortus*, other bacteria have been shown to induce PPARγ expression, such as *Mycobacterium tuberculosis* (Mahajan et al., 2012) and *Listeria monocytogenes* (Abdullah et al., 2012). Interestingly, a lack of PPARγ expression in macrophages was shown to render mice more resistant to *L. monocytogenes* infection (Abdullah et al., 2012). While the underlying mechanism in this study was not identified, our work shows that antagonizing PPARγ activity during *B. abortus* infection helps control the pathogen burden by reducing intracellular glucose availability. Importantly, these observations, together with findings by Eisele et al. (2013) demonstrating that PPARδ-dependent modulation of glucose concentration stimulates intracellular growth of *Salmonella typhimurium* in AAM, raise the possibility that PPARinduced increases in intracellular glucose availability may be a general mechanism promoting growth of persistent pathogens within AAM.

It should be noted that unlike *Francisella tularensis*, which induces differentiation of AAM to promote its replication (Shirey et al., 2008), *B. abortus* does not appear to induce this pathway directly, since cultivation of *B. abortus* with BMDM *in vitro* did not induce expression of AAM markers (Fig. S4). Rather, as a result of its inherently low TLR4-stimulatory activity for macrophages and dendritic cells (reviewed by (Martirosyan et al., 2011)), *B. abortus* induces only a weak and transient Th1 response during the acute infection phase, which is characterized by an influx of inflammatory macrophages (Fig. 1, Fig. S2A) and (Copin et al., 2012). It is likely that this transient IFNγ response is unable to sustain the CAM polarization of these cells, and perhaps together with the constant IL-4 levels throughout infection (Fig. S2B) as well as induction of IL-13 (Fig. S2C) and PPARγ during chronic infection by *B. abortus,* macrophages that have already entered the site of infection may become polarized to the AAM phenotype. Such a scenario would be consistent with our finding of similar increases in macrophage numbers during both acute and chronic infection, but a relative increase in AAM only during the chronic infection phase. These findings in the mouse model are consistent with reports of transient IFNγ responses and an increase in IL-13 producing T cells in human patients with chronic brucellosis (Rafiei et al., 2006).

Our results fit with previous reports suggesting that during chronic infection, persistent pathogens undergo a shift in their metabolism. For example, it has long been known that *M. tuberculosis* utilizes the glyoxylate shunt during intracellular infection (Wayne and Lin, 1982), and characterization of isocitrate lyase, an enzyme of this pathway needed for the chronic, but not the acute phase of infection (McKinney et al., 2000), identified this enzyme as a potential therapeutic target. Like tuberculosis, brucellosis is a chronic infection causing significant morbidity that requires protracted treatment with multiple antibiotics. Treatment failures and relapses are common for brucellosis, therefore identification of PPARγ, a well-characterized drug target, as a host factor providing a metabolic advantage to *B. abortus* during chronic infection suggests inhibitors of PPARγ as a potential adjunct to antibiotic therapy for the prevention of relapsing chronic infection.

EXPERIMENTAL PROCEDURES

Bacterial strains, media and culture conditions

Bacterial strains used in this study were the virulent strain *Brucella abortus* 2308, its isogenic mutants strain MX2 which has an insertion of pKSoriT-*bla-kan*-P*sojA-mCherry* plasmid (Copin et al., 2012), BA159 (*gluP*) which has a miniTn*5* Km2 transposon insertion interrupting the *gluP* locus (Hong et al., 2000) and BA159 complemented mutant MX6 (*gluP*::pGLUP1). For construction of strain MX6, the *gluP* gene sequence including its promoter was amplified by PCR using the primers GluP FWD: 5′-GTCGACTTTGTTGGCTTTCAAGTGG-3′ and GluP REV: 5′-GGATCCTCGCCATTCTATTCGGTTTC-3′. The resulting *gluP* PCR product was cloned into pCR2.1 using the TOPO TA cloning kit (Invitrogen, Carlsbad) and correct insertion confirmed by sequencing (SeqWright Fisher Scientific, Houston) and plasmid digestion using enzymes *Sal*I and *Bam*HI. The final construct (pGLUP1) was introduced by electroporation to strain BA159 to reconstitute the intact gene. For strain MX6, positive clones were selected based on ampicillin (Amp) resistance and intact gene chromosomal insertion was further confirmed by PCR. For strain MX2, positive clones were kanamycin (Km) resistant and fluorescent, as previously described (Copin et al., 2012). Strains were cultured on tryptic soy agar (Difco/Becton-Dickinson, Sparks, MD) or tryptic soy broth at 37°C on a rotary shaker. Bacterial inocula for mouse infection were cultured on tryptic soy agar plus 5% blood for 3 days (Alton et al., 1975). For cultures of strain MX2 and BA159, Km was added to the culture medium at 100μg/mL. All work with *B. abortus* cells was performed at biosafety level 3, and was approved by the Institutional Biosafety Committee at the University of California, Davis.

Animal experiments

Female C57BL/6J wild-type mice, *Ifng*$^{-/-}$ mice, *Ccr2*$^{-/-}$ mice and *Stat6*$^{-/-}$ mice, aged 6–8 weeks, were obtained from The Jackson Laboratory (Bar Harbor). Female and Male C57BL/6 *Pparg*$^{fl/fl}$*LysM*$^{cre/-}$ (Mac-PPARγ KO) and littermate *Pparg*$^{fl/fl}$*LysM*$^{-/-}$ (Control) mice were generated at UC Davis by mating *Pparg*$^{fl/fl}$ mice with LysM$^{cre/cre}$ mice (The Jackson Laboratory, Bar Harbor). Mice were held in microisolator cages with sterile bedding and irradiated feed in a biosafety level 3 laboratory. Groups of 4 to 6 mice were inoculated intraperitoneally (i.p.) with 0.2 mL of phosphate-buffered saline (PBS) containing 5×10^5 CFU of *B. abortus* 2308 or a 1:1 mixture of *B. abortus* 2308 and *gluP* mutant as previously described (Rolán and Tsolis, 2008). At 0, 3, 9, 15, 21, 30 and/or 60 days after infection, according to the experiment performed, the mice were euthanized by CO_2 asphyxiation and their spleens were collected aseptically at necropsy. The spleens were homogenized in 2 mL of PBS, and serial dilutions of the homogenate were plated on TSA and/or TSA+ kanamycin for enumeration of CFU. Spleen samples were also collected for gene expression, flow cytometry and immunohistochemistry analysis as described below. All animal experiments

were approved by University of California Laboratory Animal Care and Use Committee and were conducted in accordance with institutional guidelines.

Bone marrow derived macrophage infection

Bone marrow-derived macrophages were differentiated from bone marrow precursors from femora and tibiae of female, 6 to 8 weeks old, C57BL/6J mice or Mac-PPARγ KO (*Pparg*$^{-/-}$) and littermate Control (WT) mice following a previously published procedure (Rolan and Tsolis, 2007). For BMDM experiments, 24-well microtiter plates were seeded with macrophages at concentration of 5×10^5 cells/well in 0.5 mL of RPMI media (Invitrogen, Grand Island, NY) supplemented with 10% FBS and 10 mM L-glutamine (RPMI supl) incubated for 48 h at 37°C in 5% CO_2. Preparation of the inoculum and BMDM infection was performed as previously described (Rolan and Tsolis, 2007). Briefly, for inoculum preparation, *B. abortus* 2308 or *B. abortus* BA159 (*gluP*) or MX6 were grown for 24 h and then diluted in RPMI supl, and about 5×10^7 bacteria in 0.5 mL of RPMI supl were added to each well of BMDM, reaching multiplicity of infection (MOI) of 100. Microtiter plates were centrifuged at $210 \times g$ for 5 min at room temperature in order to synchronize infection. Cells were incubated for 20 min at 37°C in 5% CO_2, free bacteria were removed by three washes with phosphate-buffered saline (PBS), and the zero-time-point sample was taken as described below. After the PBS wash, RMPI supl plus 50 mg gentamicin per mL was added to the wells, and the cells were incubated at 37°C in 5% CO_2. In order to determine bacterial survival, the medium was aspirated at 0, 8, 24, and 48 h after infection according to the experiment performed, and the BMDM were lysed with 0.5 mL of 0.5% Tween 20, followed by rising of each well with 0.5 mL of PBS. Viable bacteria were quantified by serial dilution in sterile PBS and plating on TSA. For gene expression assays, BMDM were resuspended in 0.5 mL of TRI-reagent (Molecular Research Center, Cincinnati) at the time-points described above and kept at −80°C until further use. When necessary, 10 ng/mL of mouse rIFN-γ (BD Bioscience, San Jose, CA) or 10 ng/mL of mouse rIL-4 (BD Bioscience, San Jose, CA), or 3 μM of GW9662 (Cayman Ann Harbor, MI), or 5 μM of Rosiglitazone (Cayman, Ann Harbor, MI), or 50μM of Etomoxir (Sigma-Aldrich, St Louis, MO) were added to the wells overnight prior to experiment and kept throughout the experiments. All experiments were performed independently in duplicate at least four times and the standard error for each time point calculated.

CD11b$^+$ cell isolation

Macrophages (CD11b$^+$ cells) were isolated from the spleens of *B. abortus* infected C57BL/6J, congenic *Ccr2*$^{-/-}$, *Ifng*$^{-/-}$ and *Stat6*$^{-/-}$ mice with a MACS CD11b MicroBeads magnetic cell sorting kit from Miltenyi Biotech (Auburn, CA) by following the manufacturer's instructions, as previously described (Rolán et al., 2009). Briefly, single cell suspension was prepared by gently teasing apart the spleens, followed passage of splenocytes through a 70-μm cell strainer and treatment with ACK buffer (Lonza, Walkersville, MD) to lyse red blood cells. Cells were washed with PBS-BSA, counted, and incubated with CD11b MicroBeads. Cells were applied to a magnetic column, washed, eluted, and counted. For gene expression assays, total splenic CD11b$^+$ cells per mouse were resuspended in 0.5 mL of TRI-reagent (Molecular Research Center, Cincinnati) and kept at −80°C until further use. For *B. abortus* recovery essay, viable bacteria in CD11b$^-$ and CD11b$^+$ splenocytes fractions was determined by 10-fold serial dilution in sterile PBS and plating on TSA. The results were normalized to CFU per 10^6 cells.

Treatment with PPARγ agonist/antagonist *in vivo*

Female C57BL/6J mice were inoculated intraperitoneally (i.p.), daily, for 7 days prior to *B. abortus* infection, with 5mg/kg/day of the PPARγ agonist Rosiglitazone (Cayman, Ann Harbor, MI) diluted in 0.2 mL of sterile PBS solution. For the treatment with PPARγ

antagonist GW9662 (Cayman, Ann Arbor, MI), female C57BL/6J mice were inoculated intraperitoneally (i.p.), daily, from day 18 till day 30 post *B. abortus* infection, with 3mg/kg/day of PPARγ antagonist GW9662 (Cayman, Ann Arbor, MI) diluted in 0.2 mL of sterile PBS solution.

RT-PCR and real time PCR analysis

Eukaryotic gene expression was determined by real-time PCR as previously described (Rolan and Tsolis, 2007). Briefly, eukaryotic RNA was isolated using TRI reagent (Molecular Research Center, Cincinnati) according with the manufacturer's instructions. A Reverse transcriptase reaction was performed to prepare complementary DNA (cDNA) using TaqMan reverse transcription reagents (Applied Biosystems, Carlsbad CA). A volume of 4 μL of cDNA was used as template for each real-time PCR reaction in a total reaction volume of 25 μL. Real-time PCR was performed using SYBR-Green (Applied Biosystems) along with the primers listed in Table S1. Data were analyzed using the comparative Ct method (Applied Biosystems). Transcript levels of *IL-6, Nos2, Ym1, Fizz1*, *Tnfa*, *Pparg, Hifa, Pfkfb3, Glut1, Pgc1b, Acadm* and *Acadl* were normalized to mRNA levels of the housekeeping gene *act2b*, encoding β-actin.

Flow cytometry

Flow cytometry analysis for detection of CAM, AAM and/or *B. abortus* intracellular localization was performed in splenocytes and/or $CD11b^+$ splenic cells of C57BL/6J mice infected with *B. abortus* 2308 for 9 or 30 days. Briefly, after passing the spleen cells through a 100-μm cell strainer and treating the samples with ACK buffer (Lonza, Walkersville, MD) to lyse red blood cells, splenocytes were washed with PBS (Gibco) containing 1% bovine serum albumin (fluorescence-activated cell sorter [FACS] buffer). After cell counting, 4×10^6 cells/mouse were re-suspended in PBS and stained with Aqua Live/Dead cell discriminator (Invitrogen, Grand Island, NY) according to the manufacturer's protocol. After Live/Dead staining, splenocytes were resuspended in 50 μL of FACS buffer and cells were stained with cocktail of anti-B220 PE (BD Pharmigen, San Jose, CA), anti-CD3 PE (BD Pharmingen), anti-NK1.1 PE (BD Pharmigen), anti-CD11b FITC (BD Pharmingen), anti-F4/80 Pe.Cy7 (Biolegend, San Diego, CA), anti-Ly6C Pacific Blue (Biolegend), anti-Ly6G PerCP Cy5.5 (Biolegend) and anti-CD301 AF647 (AbD serotec, Raleigh, NC). The cells were washed with FACS buffer and fixed with 4% formaldehyde for 30 min at 4°C. To determine intracellular *B. abortus* localization in $CD11b^+$ splenocytes, cells were stained with cocktail of anti-CD11c PE (BD Pharmingen), anti-CD11b FITC (BD Pharmingen), anti-F4/80 Pe.Cy7 (Biolegend), anti-Ly6C Pacific Blue (Biolegend), anti-Ly6G PerCP Cy5.5 (Biolegend) and anti-CD301 AF647 (AbD Serotec), followed by cell fixation and permeabilization using Cytofix/Cytoperm (BD Pharmigen) at 4°C for 30 min. For intracellular *B. abortus* labeling, $Cd11b^+$ splenocytes were ressuspended in 50μL of Perm/Wash buffer (BD Pharmigen) and stained with APC.Cy7 (AbD Serotec) conjugated goat anti-*B. abortus* antibody followed by two washes with Perm/Wash buffer. For all experiments, cells were ressuspended in FACS buffer prior to analysis. Flow cytometry analysis was performed using an LSRII apparatus (Becton Dickinson, San Diego, CA), and data were collected for 5×10^5 cells/mouse. Resulting data were analyzed using Flowjo software (Treestar, inc. Ashland, OR). Gates were based on Fluorescence-Minus-One (FMO) controls.

Lactate measurement

For determination of extracellular lactate levels, C57BL/6J BMDM were grown in 24-well plates using RPMI media (Invitrogen, Grand Island, NY) supplemented with 2% FBS and 10 mM L-glutamine (RPMI supl) and infected as described above. At 24h post-infection, supernatants were collected and lactate measurement was performed by using a Lactate

Colorimetry Assay Kit (Biovision, Milpitas, CA) according to the manufacturer's instructions.

Glucose measurement

For determination of intracellular glucose levels, C57BL/6J BMDM were grown in 24-well plates and infected as described above. At 24h post-infection, cells were washed three times with cold PBS, and resuspended in 100 μL of glucose assay buffer. Further glucose measurement was performed by using a Glucose Assay Kit (Biovision) according to the manufacturer's instructions.

Statistical analysis

Fold changes of ratios (bacterial numbers or mRNA levels) and percentages (flow cytometry and fluorescence microscopy) were transformed logarithmically prior to statistical analysis. An unpaired Student's *t*-test was used on the transformed data to determine whether differences between groups were statistically significant ($P < 0.05$). When more than 2 treatments were used, statistically significant differences between groups were determined by one way ANOVA. All statistical analysis was performed using GraphPad Prism version 6b software (GraphPad Software, La Jolla, CA).

Supplementary Material

Refer to Web version on PubMed Central for supplementary material.

Acknowledgments

The authors are grateful to Sebastian Winter for helpful discussions during the course of this work. US PHS grants AI050553 and AI090387 to R.M.T., as well as a pilot grant from the UC Davis Proteomics Core, supported this work. T.M.A.S. was supported by a fellowship from CNPq, Brazil. Flow cytometry was performed in a facility supported by Facilities Improvement grant RR12088-01. The Animal Resources and Laboratory Services Core of the PSWRCE was supported by US PHS grant U54 AI065359.

References

Abdullah Z, Geiger S, Nino-Castro A, Böttcher JP, Muraliv E, Gaidt M, Schildberg FA, Riethausen K, Flossdorf J, Krebs W, et al. Lack of PPARg in Myeloid Cells Confers Resistance to *Listeria monocytogenes* Infection. PLoS ONE. 2012; 7:e37349. [PubMed: 22629382]

Al Dahouk S, Jubier-Maurin V, Scholz HC, Tomaso H, Karges W, Neubauer H, Kohler S. Quantitative analysis of the intramacrophagic *Brucella suis* proteome reveals metabolic adaptation to late stage of cellular infection. Proteomics. 2008; 8:3862–3870. [PubMed: 18704908]

Alton, GG.; Jones, LM.; Pietz, DE. Laboratory Techniques in Brucellosis. 2. Geneva: World Health Organization; 1975.

Barbier T, Nicolas C, Letesson JJ. *Brucella* adaptation and survival at the crossroad of metabolism and virulence. FEBS letters. 2011; 585:2929–2934. [PubMed: 21864534]

Bensinger SJ, Tontonoz P. Integration of metabolism and inflammation by lipid-activated nuclear receptors. Nature. 2008; 454:470–477. [PubMed: 18650918]

Chawla A. Control of macrophage activation and function by PPARs. Circulation research. 2010; 106:1559–1569. [PubMed: 20508200]

Copin R, Vitry MA, Hanot Mambres D, Machelart A, De Trez C, Vanderwinden JM, Magez S, Akira S, Ryffel B, Carlier Y, et al. In Situ Microscopy Analysis Reveals Local Innate Immune Response Developed around *Brucella* Infected Cells in Resistant and Susceptible Mice. PLoS Pathog. 2012; 8:e1002575. [PubMed: 22479178]

Eisele NA, Ruby T, Jacobson A, Manzanillo PS, Cox JS, Lam L, Mukundan L, Chawla A, Monack D. Persistent *Salmonella* infection is controlled by PPARδ, a host regulator of fatty acid metabolism. Cell Host Microbe. 2013 (this issue).

Essenberg RC, Candler C, Nida SK. Brucella abortus strain 2308 putative glucose and galactose transporter gene: cloning and characterization. Microbiology. 1997; 143(Pt 5):1549–1555. [PubMed: 9168605]

Fernandes DM, Jiang X, Jung JH, Baldwin CL. Comparison of T cell cytokines in resistant and susceptible mice infected with virulent *Brucella abortus* strain 2308. FEMS Immunology & Medical Microbiology. 1996; 16:193–203. [PubMed: 9116636]

Fretin D, Fauconnier A, Köhler S, Halling S, Léonard S, Nijskens C, Ferooz J, Lestrate P, Delrue RM, Danese I, et al. The sheathed flagellum of *Brucella melitensis* is involved in persistence in a murine model of infection. Cellular Microbiology. 2005; 7:687–698. [PubMed: 15839898]

Gordon S, Martinez FO. Alternative Activation of Macrophages: Mechanism and Functions. Immunity. 2010; 32:593–604. [PubMed: 20510870]

Gorvel JP, Moreno E. *Brucella* intracellular life: from invasion to intracellular replication. Veterinary Microbiology. 2002; 90:281–297. [PubMed: 12414149]

Hong PC, Tsolis RM, Ficht TA. Identification of genes required for chronic persistence of *Brucella abortus* in mice. Infection and immunity. 2000; 68:4102–4107. [PubMed: 10858227]

Kohler S, Foulongne V, Ouahrani-Bettache S, Bourg G, Teyssier J, Ramuz M, Liautard JP. The analysis of the intramacrophagic virulome of *Brucella suis* deciphers the environment encountered by the pathogen inside the macrophage host cell. Proc Natl Acad Sci U S A. 2002; 99:15711–15716. [PubMed: 12438693]

Lawrence T, Natoli G. Transcriptional regulation of macrophage polarization: enabling diversity with identity. Nature reviews Immunology. 2011; 11:750–761.

Mahajan S, Dkhar HK, Chandra V, Dave S, Nanduri R, Janmeja AK, Agrewala JN, Gupta P. *Mycobacterium tuberculosis* Modulates Macrophage Lipid-Sensing Nuclear Receptors PPARgamma and TR4 for Survival. The Journal of Immunology. 2012; 188:5593–5603. [PubMed: 22544925]

Martirosyan A, Moreno E, Gorvel JP. An evolutionary strategy for a stealthy intracellular *Brucella* pathogen. Immunological Reviews. 2011; 240:211–234. [PubMed: 21349096]

McCullough NB, Beal GA. Growth and manometric studies on carbohydrate utilization of *Brucella*. The Journal of infectious diseases. 1951; 89:266–271. [PubMed: 14888951]

McKinney JD, zu Bentrup KH, Munoz-Elias EJ, Miczak A, Chen B, Chan WT, Swenson D, Sacchettini JC, Jacobs WR, Russell DG. Persistence of *Mycobacterium tuberculosis* in macrophages and mice requires the glyoxylate shunt enzyme isocitrate lyase. Nature. 2000; 406:735–738. [PubMed: 10963599]

O'Neill LAJ, Hardie DG. Metabolism of inflammation limited by AMPK and pseudo-starvation. Nature. 2013; 493:346–355. [PubMed: 23325217]

Odegaard JI, Ricardo-Gonzalez RR, Goforth MH, Morel CR, Subramanian V, Mukundan L, Red Eagle A, Vats D, Brombacher F, Ferrante AW, et al. Macrophage-specific PPARgamma controls alternative activation and improves insulin resistance. Nature. 2007; 447:1116–1120. [PubMed: 17515919]

Rafiei A, Ardestani SK, Kariminia A, Keyhani A, Mohraz M, Amirkhani A. Dominant Th1 cytokine production in early onset of human brucellosis followed by switching towards Th2 along prolongation of disease. Journal of Infection. 2006; 53:315–324. [PubMed: 16488475]

Reyes JL, Terrazas LI. The divergent roles of alternatively activated macrophages in helminthic infections. Parasite Immunology. 2007; 29:609–619. [PubMed: 18042168]

Rolan HG, Tsolis RM. Mice lacking components of adaptive immunity show increased *Brucella abortus virB* mutant colonization. Infection and immunity. 2007; 75:2965–2973. [PubMed: 17420243]

Rolán HG, Tsolis RM. Inactivation of the Type IV Secretion System Reduces the Th1 Polarization of the Immune Response to *Brucella abortus* Infection. Infection and immunity. 2008; 76:3207–3213. [PubMed: 18458071]

Rolán HG, Xavier MN, Santos RL, Tsolis RM. Natural Antibody Contributes to Host Defense against an Attenuated *Brucella abortus virB* Mutant. Infection and immunity. 2009; 77:3004–3013. [PubMed: 19364836]

Shi C, Pamer EG. Monocyte recruitment during infection and inflammation. Nature reviews Immunology. 2011; 11:762–774.

Shirey KA, Cole LE, Keegan AD, Vogel SN. *Francisella tularensis* Live Vaccine Strain Induces Macrophage Alternative Activation as a Survival Mechanism. The Journal of Immunology. 2008; 181:4159–4167. [PubMed: 18768873]

Starr T, Ng TW, Wehrly TD, Knodler LA, Celli J. *Brucella* Intracellular Replication Requires Trafficking Through the Late Endosomal/Lysosomal Compartment. Traffic. 2008; 9:678–694. [PubMed: 18266913]

Szanto A, Balint BL, Nagy ZS, Barta E, Dezso B, Pap A, Szeles L, Poliska S, Oros M, Evans RM, et al. STAT6 transcription factor is a facilitator of the nuclear receptor PPARgamma-regulated gene expression in macrophages and dendritic cells. Immunity. 2010; 33:699–712. [PubMed: 21093321]

Van Dyken SJ, Locksley RM. Interleukin-4- and Interleukin-13-Mediated Alternatively Activated Macrophages: Roles in Homeostasis and Disease. Annual Review of Immunology. 2013; 31 null.

Vats D, Mukundan L, Odegaard JI, Zhang L, Smith KL, Morel CR, Wagner RA, Greaves DR, Murray PJ, Chawla A. Oxidative metabolism and PGC-1beta attenuate macrophage-mediated inflammation. Cell metabolism. 2006; 4:13–24. [PubMed: 16814729]

Wayne LG, Lin KY. Glyoxylate metabolism and adaptation of *Mycobacterium tuberculosis* to survival under anaerobic conditions. Infection and immunity. 1982; 37:1042–1049. [PubMed: 6813266]

Xavier MN, Paixão TA, Poester FP, Lage AP, Santos RL. Pathological, Immunohistochemical and Bacteriological Study of Tissues and Milk of Cows and Fetuses Experimentally Infected with *Brucella abortus*. Journal of Comparative Pathology. 2009; 140:149–157. [PubMed: 19111839]

Yki-Järvinen H. Thiazolidinediones. New England Journal of Medicine. 2004; 351:1106–1118. [PubMed: 15356308]

Highlights

- Persistent *Brucella abortus* is associated with alternatively activated macrophages (AAM)
- PPARγ increases glucose availability to promote intracellular *B. abortus* replication in AAM
- *B. abortus* persistent infection depends on the bacterium's ability to transport glucose
- PPARγ activation contributes to increased persistence of *B. abortus in vivo*

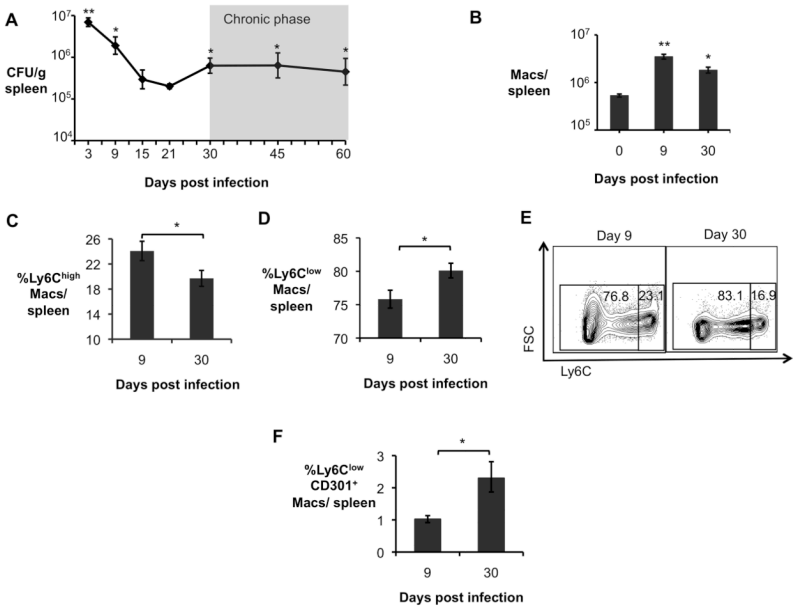

Figure 1. Alternatively activated macrophages are more abundant during chronic brucellosis

(A) *B. abortus* 2308 CFU counts in spleens from C57BL/6J mice (n=5) at 3, 9, 15, 21, 30, 45 and 60 days post infection (d.p.i). **(B)** Numbers of macrophages ($CD3^-B220^-NK1.1^-Ly6G^-CD11b^+F4/80^+$) determined by flow cytometry in spleens of *B. abortus* infected mice (n=4) at 0, 9 and 30 d.p.i. **(C)** Frequency of $CD3^-B220^-NK1.1^-Ly6G^-CD11b^+F4/80^+Ly6C^{high}$ macrophages (CAM) measured by flow cytometry in spleens of *B. abortus* infected mice (n=4) at 9 and 30 d.p.i.. **(D)** Frequency of $CD3^-B220^-NK1.1^-Ly6G^-CD11b^+F4/80^+Ly6C^{low}$ macrophages determined by flow cytometry in spleens of *B. abortus* infected mice (n=4) at 9 and 30 d.p.i. **(E)** Representative data plot of $Ly6C^{low}$ and $Ly6C^{high}$ populations in spleens of *B. abortus* infected mice at 9 and 30 d.p.i.. **(F)** Frequency of $CD3^-B220^-NK1.1^-Ly6G^-CD11b^+F4/80^+Ly6C^{low}CD301^+$ macrophages (AAM) measured by flow cytometry in spleens of *B. abortus* infected mice (n=4) at 9 and 30 d.p.i.. Values represent mean ± SEM. (*) Represents $P<0.05$ and (**) represents $P<0.01$ using one way ANOVA for (A–B) or unpaired t-test analysis for (C–E). See also Fig. S1.

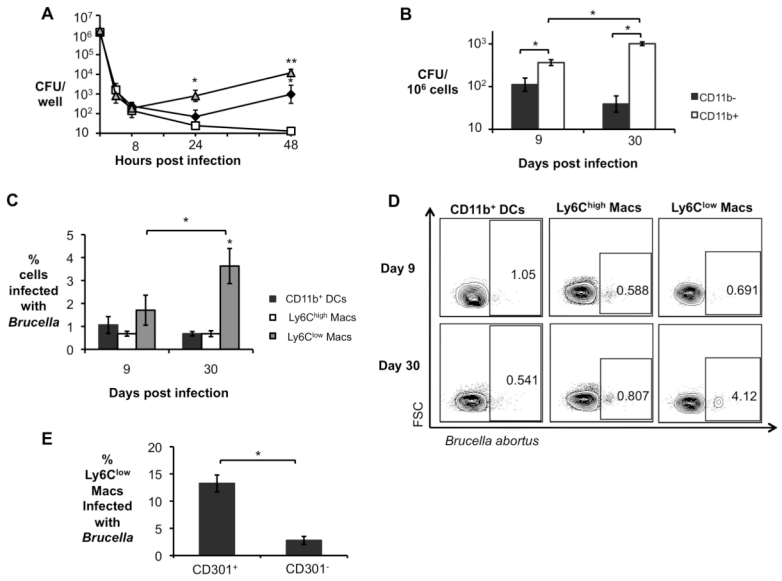

Figure 2. Increased *B. abortus* survival in AAM during chronic infection

(A) *B. abortus* survival over time in C57BL/6J BMDM that were not treated (black diamond), or stimulated with 10ng/mL of rIFNγ (CAM, open square) and stimulated with 10ng/mL of rIL-4 (AAM, grey triangle). Data shown are compiled from four independent experiments. **(B)** *B. abortus* 2308 CFU counts in $CD11b^-$ and $CD11b^+$ splenocytes from C57BL/6J mice (n=5) at 9 and 30 days post infection (d.p.i.). **(C)** Frequency *of B. abortus* infected $CD11b^+$ dendritic cells (DCs, $F4/80^-Ly6G^-$ $CD11b^+CD11c^+$), $Ly6C^{high}$ macrophages ($CD11c^-Ly6G^-CD11b^+F4/80^+Ly6C^{high}$) and $Ly6C^{low}$ macrophages ($CD11c^-Ly6G^-CD11b^+F4/80^+Ly6C^{low}$) determined by flow cytometry in $CD11b^+$ splenocytes from infected C57BL/6J mice (n=5) at 9 and 30 d.p.i. **(D)** Representative data plot of populations shown in (C). **(E)** Frequency of *B. abortus* infected $CD301^+$ (AAM) and $CD301^-$ $Ly6C^{low}$ macrophages in $CD11b^+$ splenocytes determined by flow cytometry in $CD11b^+$ splenocytes from C57BL/6J infected mice (n=5) at 30 d.p.i. Values represent mean ± SEM. (*) Represents $P<0.05$ and (**) represents $P<0.01$ using one way ANOVA for (A) or unpaired t-test analysis for (B–C) and (E).

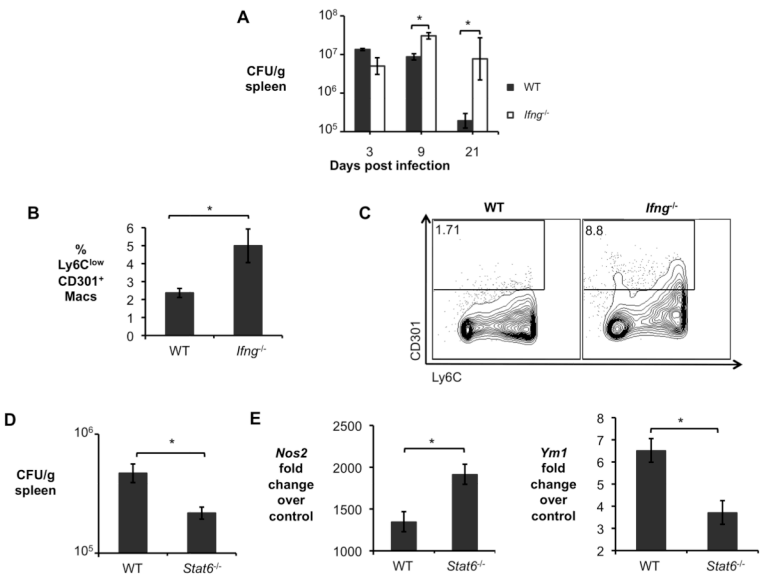

Figure 3. Defects in generation of CAM or AAM affect *B. abortus* survival *in vivo*

(A) *B. abortus* 2308 CFU counts in spleens from C57BL/6J and congenic *Ifng*$^{-/-}$ mice (n=5) at 3, 9, and 21, days post infection (d.p.i). **(B)** Frequency of CD3^{-}B220^{-}NK1.1^{-}Ly6G^{-}CD11b^{+}F4/80^{+}Ly6C^{low}CD301^{+} macrophages (AAM) measured by flow cytometry in spleens of *B. abortus* infected C57BL/6J and congenic *Ifng*$^{-/-}$ mice (n=5) at 9 d.p.i.. **(C)** Representative data plot of populations shown in (B). **(D)** *B. abortus* 2308 CFU counts in spleens of C57BL/6J and congenic *Stat6*$^{-/-}$ mice (n=5) at 30 d.p.i. **(E)** Real time RT-PCR gene expression analysis of CAM gene *Nos2* and AAM gene *Ym1* in CD11b^{+} splenocytes from *B. abortus* infected C57BL/6J and congenic *Stat6*$^{-/-}$ mice (n=5) at 30 d.p.i. Values represent mean ± SEM. (*) Represents P<0.05 using unpaired t-test statistical analysis. See also Fig. S2.

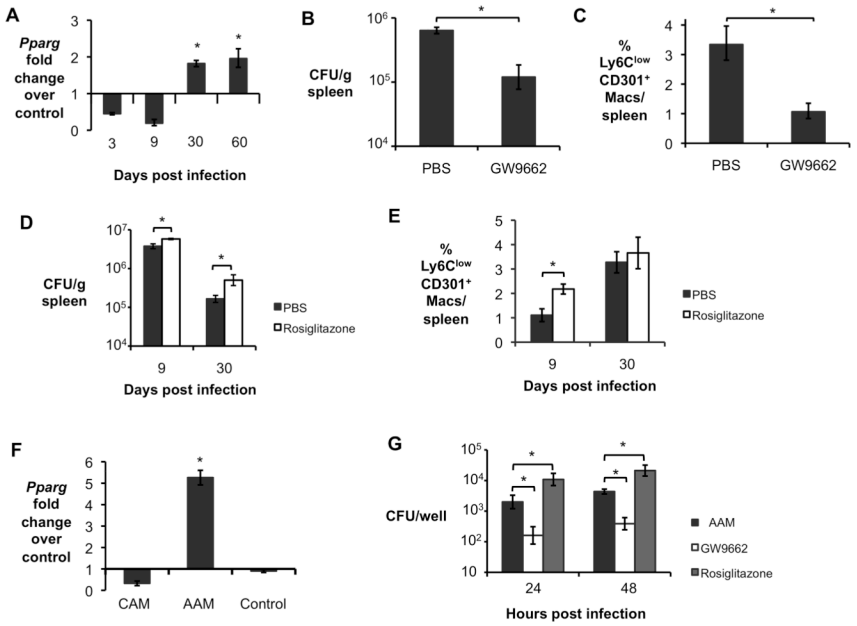

Figure 4. Increased survival of *B. abortus* during chronic infection is dependent on PPARγ

(A) Real time RT-PCR gene expression analysis of *Pparg* in $CD11b^+$ splenocytes from *B. abortus*-infected C57BL/6J mice (n=5) at 3, 9, 30 and 60 dpi. **(B)** *B. abortus* 2308 CFU counts, measured at 30 d.p.i., in spleens from C57BL/6J mice (n=5) treated daily from 18 to 30 d.p.i. with PPARγ antagonist GW9662 or PBS control. **(C)** Frequency of $CD3^-B220^-NK1.1^-Ly6G^-CD11b^+F4/80^+Ly6C^{low}CD301^+$ macrophages (AAM) measured by flow cytometry at 30 d.p.i. in spleens of C57BL/6J mice (n=5) treated daily from 18 to 30 d.p.i. with PPARγ antagonist GW9662 or PBS control. **(D)** *B. abortus* 2308 CFU counts, measured at 9 and 30 d.p.i., in spleens from C57BL/6J mice (n=5) treated daily for 7 days prior to infection with PPARγ agonist Rosiglitazone or PBS control. **(E)** Frequency of $CD3^-B220^-NK1.1^-Ly6G^-CD11b^+F4/80^+Ly6C^{low}CD301^+$ macrophages (AAM) measured by flow cytometry at 9 and 30 d.p.i. in spleens from C57BL/6J mice (n=5) treated daily for 7 days prior to infection with PPARγ agonist Rosiglitazone or PBS control. **(F)** Real time RT-PCR gene expression analysis of *Pparg* in BMDM from C57BL/6J mice stimulated with rIFN-γ (CAM), rIL-4 (AAM), or non-stimulated (Control) and infected with *B. abortus* for 24h. Data shown are compiled from four independent experiments. **(G)** *B. abortus* 2308 CFU counts in BMDM from C57BL/6J mice, stimulated with rIL-4 (AAM) or with IL-4 + 3μM of PPARγ antagonist GW9662 (GW9662) or with 5μM of PPARγ agonist Rosiglitazone and infected with *B. abortus* for 24 and 48h. Data shown in (F) and (G) are compiled from four independent experiments. Values represent mean ± SEM. (*) Represents $P<0.05$ using one way ANOVA for (A) and (F) or unpaired t-test analysis for (B–E) and (G). See also Fig. S3.

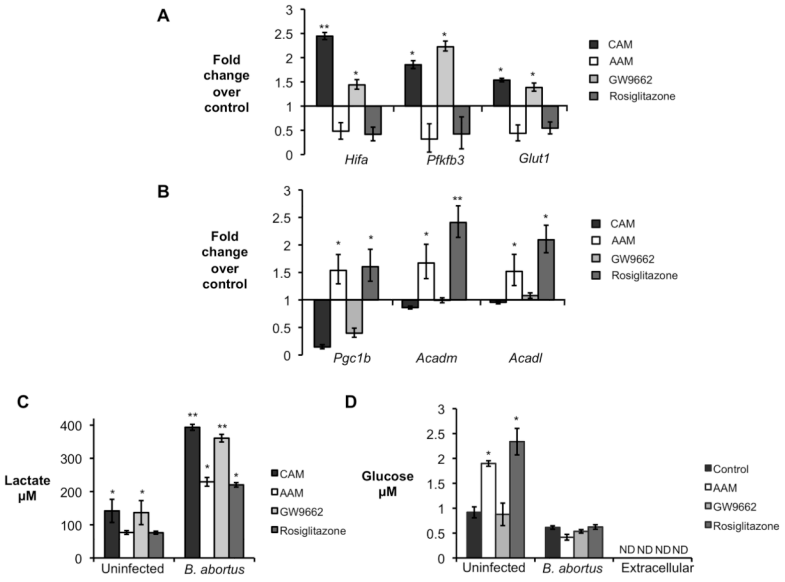

Figure 5. *B. abortus* infected AAM exhibit a PPARγ-dependent decrease in glycolytic metabolism

(A) Real time RT-PCR gene expression analysis of glycolytic pathway genes *Hifa* (hypoxia inducible factor α), *Pfkfb3* (phosphofructokinase-3) and *Glut1* (glucose transporter 1) in C57BL/6J BMDM stimulated with rIFNγ (CAM), with rIL-4 (AAM), with IL-4 + GW9662 (GW9662) or with Rosiglitazone and infected with *B. abortus* for 8 hours. Results are expressed as fold change over untreated macrophages infected with *B. abortus*. **(B)** Real time RT-PCR gene expression analysis of fatty acid β-oxidation pathway genes *Pgc1b* (PPARγ coactivator 1 β), *Acadm* (medium-chain acyl-CoA dehydrogenase) and *Acadl* (long-chain acyl-CoA dehydrogenase) in BMDM from C57BL/6J stimulated rIFNγ (CAM), with rIL-4 (AAM), with IL-4 + GW9662 (GW9662) or with Rosiglitazone and infected with *B. abortus* for 8 hours. Results are expressed as fold change over untreated macrophages infected with *B. abortus*. **(C)** Measurement of lactate concentration in supernatant from BMDM from C57BL/6J stimulated with rIFNγ (CAM), with rIL-4 (AAM) or IL-4 + GW9662 (GW9662) or with Rosiglitazone and uninfected or infected with *B. abortus* for 24 hours. **(D)** Measurement of intracellular glucose concentration in BMDM from C57BL/6J unstimulated (control) and stimulated with rIL-4 (AAM), with IL-4 + GW9662 (GW9662), or with Rosiglitazone and uninfected or infected with *B. abortus* for 24 hours. Values represent mean ± SEM and represent combined results of four independent experiments conducted in duplicate. (*) Represents P<0.05 and (**) represents P<0.01 using one way ANOVA. See also Fig. S4.

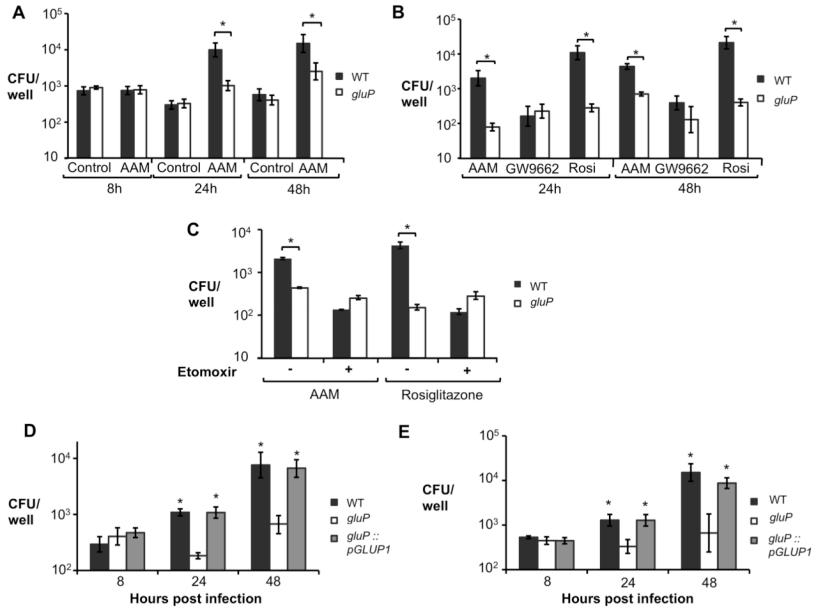

Figure 6. A PPARγ-dependent increase in intracellular glucose availability promotes survival of *B. abortus* in macrophages

(A) Recovery of *B. abortus* from C57BL/6J BMDM that were sham-treated (Control) or treated with rIL-4 (AAM). BMDM were infected with *B. abortus* 2308 WT or isogenic *gluP* mutant for 8, 24 and 48h. **(B)** Recovery of *B. abortus* from C57BL/6J BMDM stimulated with rIL-4 (AAM), with IL-4 + GW9662 (GW9662) or with Rosiglitazone (Rosi) and infected with *B. abortus* 2308 (WT) or isogenic *gluP* mutant for 24 and 48h. **(C)** Recovery of *B. abortus* from BMDM from C57BL/6J treated or not with the β-oxidation inhibitor etomoxir (50 μM) in the presence of rIL-4 (AAM) or Rosiglitazone and infected with *B. abortus* 2308 WT or isogenic *gluP* mutant for 48h. **(D)** Recovery of *B. abortus* from BMDM from C57BL/6J stimulated rIL-4 (AAM) and infected with *B. abortus* 2308 WT or isogenic *gluP* mutant or complemented *gluP* mutant (*gluP*::pGLUP1) for 8, 24 and 48h. **(E)** Recovery of *B. abortus* from BMDM from C57BL/6J stimulated with Rosiglitazone and infected with *B. abortus* 2308 WT or isogenic *gluP* mutant or complemented *gluP* mutant (*gluP*::pGLUP1) for 8, 24 and 48h. Values represent mean ± SEM of data from four independent experiments conducted in duplicate. (*) Represents $P<0.05$ using unpaired t-test for (A–C) or one way ANOVA statistical analysis for (D–E). See also Fig S5.

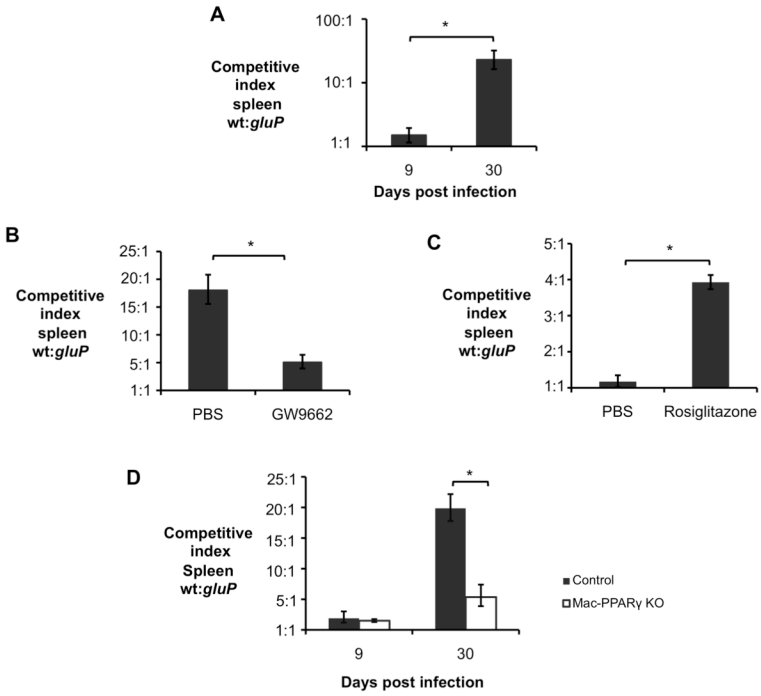

Figure 7. A PPARγ-dependent increase in intracellular glucose availability in macrophages promotes *B. abortus* persistence *in vivo*

(A) Competitive index (ratio of WT to *gluP* mutant) in spleens of C57BL/6J mice (n=5) infected with a 1:1 mixture of *B. abortus* 2308 WT and isogenic *gluP* mutant for 9 and 30 days. **(B)** Competitive index, measured at 30 days post infection (d.p.i.), in spleens from C57BL/6J mice (n=5) treated daily from 18 to 30 d.p.i. with PPARγ antagonist GW9662 or PBS control and infected with a 1:1 mixture of *B. abortus* 2308 WT and isogenic *gluP* mutant. **(C)** Competitive index, measured at 9 and 30 d.p.i., in spleens from C57BL/6J mice (n=5) treated daily for 7 days prior to infection with PPARγ agonist Rosiglitazone or PBS control and infected with a 1:1 mixture of *B. abortus* 2308 WT and isogenic *gluP* mutant. **(D)** Competitive index, measured at 9 and 30 d.p.i., in spleens from $Pparg^{fl/fl}LysM^{cre/-}$ (Mac-PPARγ KO) or littermates $Pparg^{fl/fl}LysM^{-/-}$ (Control) mice (n=5) infected with a 1:1 mixture of *B. abortus* 2308 WT and isogenic *gluP* mutant. Values represent mean ± SEM. (*) Represents $P<0.05$ using unpaired t-test statistical analysis.